Steady-State Numerical Simulation of a Fin-and-Tube Evaporator

Harshit Dhiman

January 22, 2026

1 Abstract

This report outlines the development of a steady-state finite volume solver to calculate the performance of a multi-pass fin and tube evaporator. The model predicts cooling capacity, pressure drops and the spatial temperature distributions across the heat exchanger. The evaporator tubes are discretized into one-dimensional control volumes, within which the steady-state mass, momentum, and energy conservation equations are solved.

Nomenclature

A_c	Minimum free flow area
A_o	Total outer area
B_o	Boiling number
C_o	Convection number
C_p	Specific heat capacity at constant pressure
D_c	Outer diameter of fin collar
ΔP	Pressure Drop (Pa)
D_h	Hydraulic diameter
f	Friction Factor
F_{fl}	Fluid dependent parameter
F_p	Fin pitch
Fr_{lo}	Froud number with all flow as liquid
G_c	Mass flux based on the minimum area
h	Heat Transfer Coefficient
i_{lg}	Latent heat of vapourization
j	Colburn Factor
N	Number of rows in the direction of air flow
P_l	Longitudinal pitch
Pr	Prandtl number
P_t	Transverse pitch
Re	Reynold's number
ρ	Density

2 Introduction

2.1 Objective

The objective is to build a numerical solver to simulate a multi-pass fin and tube evaporator operating under sub-critical conditions. The model aims to:

- Simulate steady state operation under specified inlet air and refrigerant conditions.
- Accurately capture the spatial transition from two phase mixture to single phase superheated vapour.
- Quantify total cooling capacity, pressure drop and the outlet temperature of the refrigerant accounting for latent heat loads for wet coil conditions.

2.2 Engineering Challenges

The development of this solver addressed several non-linear phenomena inherent in an evaporator:

- **Two-phase flow**: The flow inside an evaporator is two-phase for most of its length. Analytical methods like the LMTD method are insufficient for phase change in flow. The solver uses a 1-D finite volume approach instead of a lumped model to accommodate this change.
- **Coupled Heat Balance**: The solution requires solving the implicit energy balance equation where the wall temperature is unknown and is dependent on both the fluid states.
- **Regime-Dependent Physics**: The heat transfer coefficient changes drastically with vapour quality. The solver must handle the discontinuity when switching from two-phase boiling to single phase convection.
- **Variable Fluid Properties**: The fluid properties in the two-phase region especially near the saturation line is non-linear, hence constant properties cannot be assumed. The solver uses real-fluid data driven equations of state via CoolProp to capture this non-linearity.

3 Methodology: Physical Model

3.1 Geometric Parametrization

The simulation employs a fully parametric design approach, decoupling the physical geometry from the numerical solver. The geometric and thermodynamic parameters are ingested form an external JSON file. This allows the tool to be used for rapid geometric iterations without changing the source code.

3.1.1 Geometric Definition

The heat exchanger is defined as a staggered fin and tube arrangement. The primary geometric constraints are described below:

- The fin profile is plain, which is hard-coded into the solver. Future plans include expanding the solver to be able to solve for louvered fins as well.
- **Tube Matrix**: Defined by the number of tube rows (N), number of holes per row, the longitudinal pitch (P_l) and the transverse pitch (P_t).
- **Fin Geometry**: Characterized by the fin pitch (F_p), the fin thickness δ_t and the finned length.
- **Tube Geometry**: Defined by the outer diameter of the tube (D_o), the tube wall thickness and the inner wall surface type. The solver assumes a smooth inner wall surface type. Future plans include expanding the solver to incorporate inner grooved tubes (IGT).

3.1.2 Derived Characteristic Parameters

To ensure the compatibility with empirical heat transfer correlations, the solver pre-calculates derived geometric constraints based on the primary geometric inputs.

- **Fin Collar Diameter (D_c)**: Calculated as the tube OD plus twice the fin thickness ($OD + 2\delta_f$), used as the characteristic length for air-side Reynolds number calculations.
- **Hydraulic Diameter (D_h)**: Computed based on the ratio of net free volume to wetted surface area.
- **Surface Area Analysis**: The code automatically computes the total primary (tube) and secondary (fin) surface areas (A_o), as well as the minimum free-flow cross-sectional area (A_c), which is critical for determining maximum air mass flux (G_c).

3.1.3 Operational Boundary Conditions

Operational parameters are treated as variable state inputs, distinct from the fixed geometric core. This includes boundary conditions such as volumetric air flow ($\dot{V}_{air}$), inlet air thermodynamic state (Temperature and Relative Humidity), refrigerant mass flux ($\dot{m}_{ref}$), and saturation pressure. This separation allows the solver to evaluate the performance of a fixed geometric design under varying load conditions and flow regimes.

3.2 Air Side Correlations

The air side heat transfer is solved using the **Wang et al. (2000)**[1] correlations to determine the Colburn j - factor and the friction factor f, which are in-turn used to solve for the air side heat transfer coefficient and pressure drop.

The relationships are given below:

$$j = 0.086 \cdot Re_{D_c}^{P3} \cdot N^{P4} \cdot \left(\frac{F_p}{D_c}\right)^{P_5} \cdot \left(\frac{F_p}{D_h}\right)^{P_6} \cdot \left(\frac{F_p}{P_t}\right)^{-0.93} \tag{1}$$

$$f = 0.0267 \cdot Re_{D_c}^{F1} \cdot \left(\frac{P_t}{P_l}\right)^{F2} \cdot \left(\frac{F_p}{D_c}\right)^{F3} \tag{2}$$

These relations are then used to calculate the heat transfer coefficient and the pressure drop for the air side of the heat exchanger. The eq (3) is based on the definition of the Colburn factor. The pressure drop equation is used as proposed by **Kays and London**[2] The air density across the heat exchanger is considered to be constant reducing the equation to eq (4).

$$h_{air} = \frac{j \cdot G_c \cdot C_{p,air}}{Pr_{air}^{2/3}} \tag{3}$$

$$\Delta P = f \cdot \frac{A_o}{A_c} \cdot \frac{G_c^2}{2\rho} \tag{4}$$

3.3 Refrigerant side correlations

The in-tube evaporation heat transfer coefficient is calculated using the general correlation proposed by **Kandlikar (1990)**[3] . This method explicitly accounts for the competition between nucleate boiling and convective boiling mechanisms.

The two-phase heat transfer coefficient h_{TP} is the larger of the values calculated for the nucleate boiling region (h_{nb}) and the convective boiling region (h_{cb}):

$$h_{TP} = \max(h_{nb}, h_{cb}) \tag{5}$$

The governing equations for the two regions are:

$$h_{nb} = h_l \left[0.6683 Co^{-0.2} (25 Fr_{lo})^{0.3} + 1058 Bo^{0.7} F_{fl}\right] \tag{6}$$

$$h_{cb} = h_l \left[1.136 Co^{-0.9} (25 Fr_{lo})^{0.3} + 667.2 Bo^{0.7} F_{fl}\right] \tag{7}$$

Where:

- Co: Convection number $\left(\frac{1-x}{x}\right)^{0.8} \left(\frac{\rho_v}{\rho_l}\right)^{0.5}$
- Bo: Boiling number $\frac{q''}{Gi_{fg}}$

- Fr_{lo}: Froude number with all flow as liquid
- F_{fl}: Fluid-dependent parameter (Used $F_{fl} = 3.3$ for R32/Copper[4])

3.3.1 Pressure drop formulation

The hydraulic resistance within the evaporator coil is modelled as a superposition of two distinct physical mechanisms: frictional losses due to wall shear and inter-facial stress, and momentum changes due to flow acceleration.

Frictional Pressure Drop (Friedel Correlation): The frictional pressure gradient in the two-phase region is evaluated using the correlation proposed by **Friedel (1979)**[5] . This model was selected for its proven robustness in horizontal flow regimes typical of HVAC evaporators, particularly where stratified-wavy flow may occur. The model employs a "separate flow" multiplier approach, where the two-phase pressure drop is calculated by scaling the pressure drop of the liquid phase flowing alone:

$$\left(\frac{dp}{dz}\right)_{2\phi} = \Phi_{lo}^2 \cdot \left(\frac{dp}{dz}\right)_{lo} \tag{8}$$

Where $\left(\frac{dp}{dz}\right)_{lo}$ is the pressure gradient assuming the total mass flow circulates as liquid, and Φ_{lo}^2 is the two-phase multiplier. The solver computes this multiplier dynamically based on the local vapour quality (x), incorporating dimensionless groups to capture the balance of forces:

- Froude Number (Fr): accounts for gravity forces (stratification effects).
- Weber Number (We): accounts for surface tension forces (bubble formation and breakup).

The comprehensive Friedel multiplier is computed as:

$$\Phi_{lo}^2 = E + \frac{3.24FH}{Fr^{0.045}We^{0.035}} \tag{9}$$

(Where E, F, and H are dimensionless property and quality factors defined in the source code).

Momentum Pressure Drop (Acceleration Head): As the refrigerant evaporates, the dramatic difference in density between the liquid and vapour phases ($\rho_v \ll \rho_l$) forces the flow to accelerate to satisfy mass continuity. This acceleration results in a "momentum pressure drop" that is non-negligible in high-heat-flux evaporators. The solver quantifies this by evaluating the change in momentum flux (M) across each control volume:

$$\Delta P_{mom} = G^2 \left(M_{out} - M_{in}\right) \tag{10}$$

The momentum flux M is defined as:

$$M = \frac{(1-x)^2}{\rho_l(1-\alpha)} + \frac{x^2}{\rho_v \alpha} \tag{11}$$

Where α represents the void fraction. For this implementation, the Homogeneous Equilibrium Model (HEM) is used to approximate the void fraction, assuming equal velocities (zero slip) between the liquid and vapour phases.

Total Hydraulic Resistance: The total pressure drop for each discretized segment is the summation of these components:

$$\Delta P_{total} = \Delta P_{fric} + \Delta P_{mom} \tag{12}$$

This coupled approach ensures that the simulation accounts for the "pressure glide" effect, where the saturation temperature (T_{sat}) drops along the tube length as pressure decreases, directly impacting the effective driving temperature difference.

4 Methodology: Numerical Model

4.1 Discretization strategy

The heat exchanger is modelled as a 1D tube which is discretized into finite number of control volumes whose number is controlled by user input. The elements are equal partitions of the HX tube each of length dl. The heat transfer is solved by formulating the energy balance at each length segment while stepping forward through the length of the tube. The thermodynamic properties and state variables are calculated using `CoolProp` python wrapper.

4.2 Energy Balance

The inner loop of the solver computes the wall temperature by finding the root of the energy balance equation:

$$h_{ref} A_i (T_{wall} - T_{ref}) - h_{air} A_o (T_{air} - T_{wall}) = 0$$

The iterative routine follows these steps:

- **Initialization**: A trial value for the wall temperature, T_{wall}, is generated by the solver.
- **Air-Side Calculation**: The heat transfer rate is calculated using the established air-side heat transfer coefficient, h_{air}.
- **Refrigerant-Side Coupling**: The resulting heat flux is used to compute the Boiling number (Bo), which updates the refrigerant heat transfer coefficient, h_{ref}.
- **Convergence**: The solver evaluates the residual energy imbalance. The precise root is located using Brent's method, implemented using the `scipy.optimize.root_scalar` function.

The core loop of the root finding algorithm is shown below.

```
# From evap.py
def err(T_wall_guess):
    Qguess = h_air * A_o * (T_air - T_wall_guess)
    Qref = h_ref * A_i * (T_wall_guess - T_ref)
    return Qguess - Qref

sol = root_scalar(err, bracket=[T[u], localAirTemp[u]], method="brentq")
Twall = sol.root
Qref = h_ref * (math.pi * tubeID * dl) * (Twall - T[u]) # heat transfer for the
    specific segment.
```

Listing 1: Root finding algorithm for Wall Temperature

The solver iterates through the tube length, and updates the refrigerant state at each step. The enthalpy update for the next step is done as shown below in Equation (13)

$$H_{i+1} = H_i + \frac{dQ_{segment}}{\dot{m}_{ref}} \tag{13}$$

4.3 Air side temperature

The solver assumes the HX to have more than 2 rows in the direction of air flow. The temperature of air changes at each row, thus changing the amount of heat transferred in that row. To account

for this, the outer loop of the solver iteratively solves for the local temperature of the air, stores the temperature profile and uses that for the calculation of the heat transfer in the inner loop. The temperature change is calculated using an effective specific heat capacity ($C_{p,eff}$) of $2000 J/kg \cdot K$ to account for the latent heat loads when inlet air RH is greater than 0.4. The loop is run for 5 iterations by default which is usually enough for convergence.

```
# From evap.py
step = nIter // nRows
    localAirTemp[(nRows - 1) * step :] = inletAirTemp

    for p in range(nRows - 1, 0, -1):
        upwind_start = p * step
        upwind_end = (p + 1) * step

        downwind_start = (p - 1) * step
        downwind_end = p * step

        for k in range(step):

            idx_upwind = upwind_start + k
            idx_downwind = downwind_start + k

            Cp_eff = 2000.0 if inletAirRH > 0.4 else 1006.0

            dT_air = QperSegment[idx_upwind] / (mDotPerSegment * Cp_eff)

            localAirTemp[idx_downwind] = localAirTemp[idx_upwind] - dT_air
```

Listing 2: Air side grid update algorithm

4.4 Logic Flowchart

The following diagram (Figure 1) illustrates the logic flow of the solver.

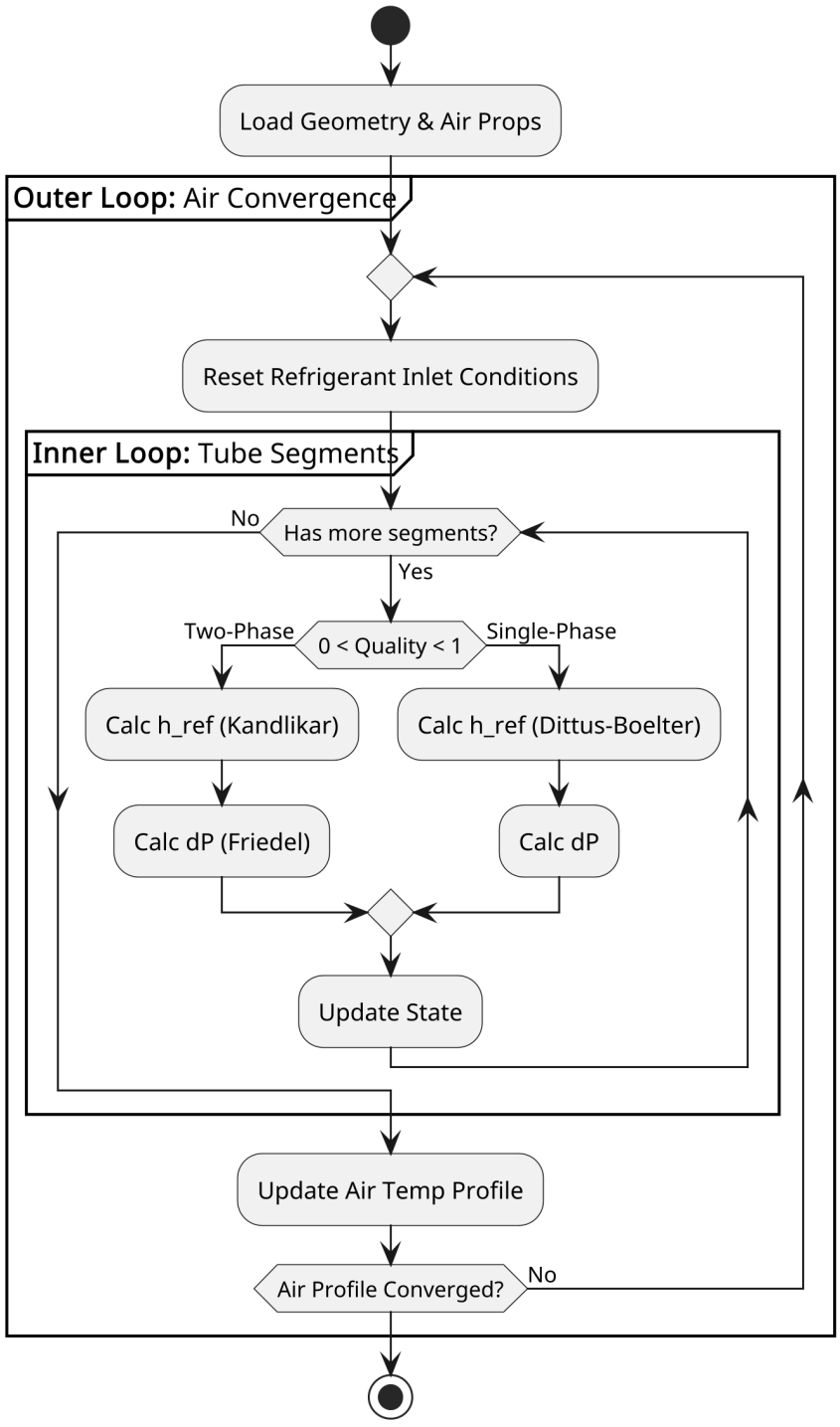

Figure 1: Logic flow diagram for the solver

5 Results and Discussion

5.1 Model Inputs

To test and validate the solver, a test case is run which is defined in an external file (`evapProps.json`). The specific parameters used are given in Table 1

Table 1: Input Parameters

Parameter name	Value
Number of elements	1000
No. of rows	2
No. of Holes per row	12
Transverse Pitch (mm)	21
Longitudinal Pitch (mm)	16.5
Tube OD (mm)	7.4
Tube Thickness (mm)	0.28
Fin Thickness	0.12
Fin Pitch (mm)	2.2
Finned Length (mm)	600
Refrigerant	R32
Operating Pressure (psi)	110
Inlet Air RH (fraction)	0.5
Inlet Air Temp (°C)	35
Volumetric Air flow (m^3/h)	2000
Atmospheric Pressure (psi)	14.7
Inlet Quality (fraction)	0.21
Refrigerant Flow Rate (kg/s)	0.0141

5.2 Thermodynamic Preformance Analysis

5.2.1 P-h Analysis

The global thermodynamic behaviour of the evaporator is analysed by mapping the state points of each discretized control volume onto a Pressure-Enthalpy (P-h) diagram. This visualisation serves as the primary validation step for the simulation, confirming that the refrigerant evolution follows the expect cycle constraints. The P-h diagram generated is shown in Figure 2

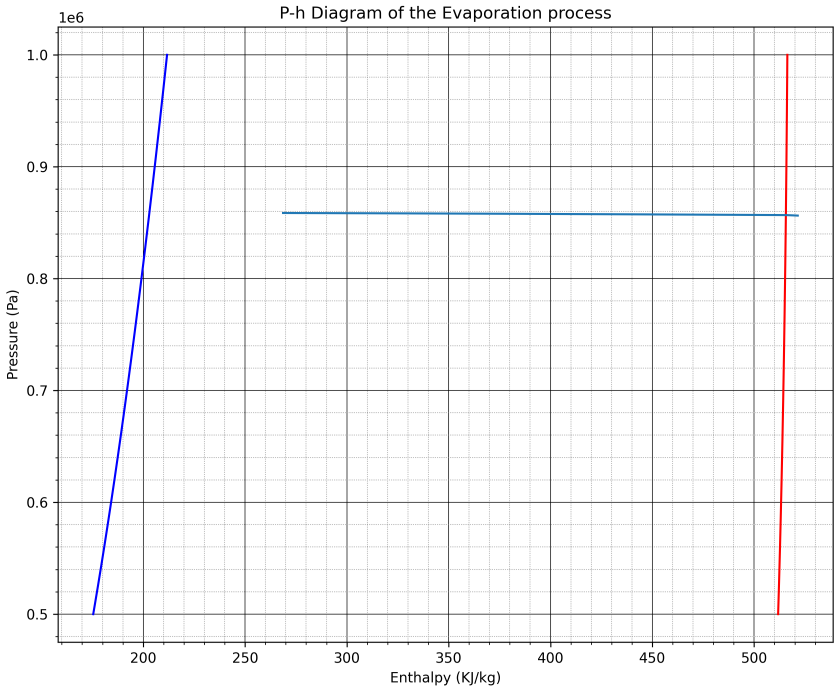

Figure 2: Pressure-Enthalpy diagram of the evaporation process

The generated $P - h$ plot explicitly visualizes the non-isobaric evaporation process. Unlike idealized theoretical cycles, the simulation captures the hydraulic pressure penalty associated with flow through the tube bank. The "glide" or downward slope of the process line within the two-phase region indicates the total pressure drop (ΔP_{total}), which is a summation of frictional losses and momentum pressure changes calculated at each iterative step.

5.2.2 Phase Evolution and Superheat

The transition from the two-phase saturation region to superheated vapour is identified by mapping the spatial evolution of vapour quality (x) along the tube length. The plot is shown in Figure 3

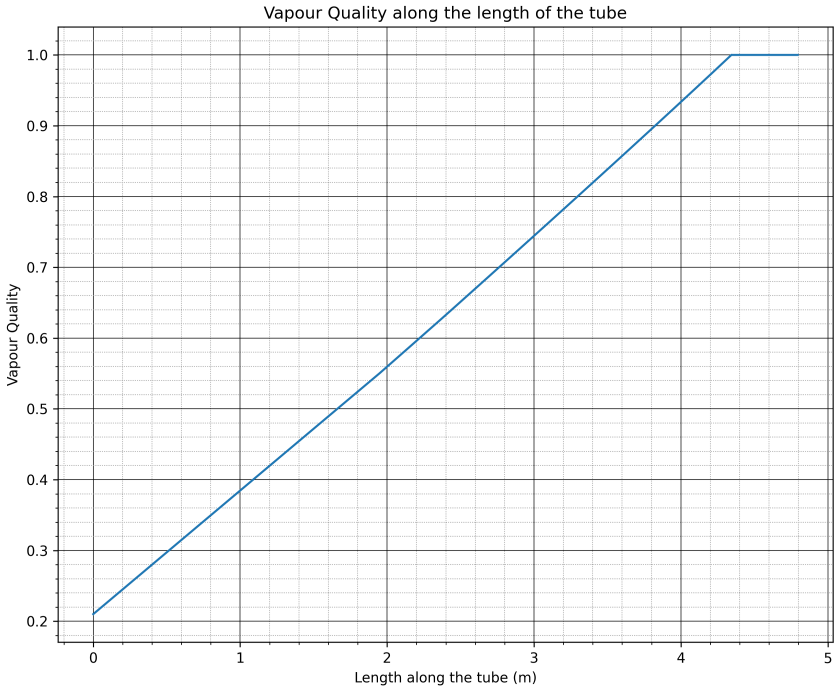

Figure 3: Vapour Quality along the length of the tube

- Two-Phase Region: The majority of the heat transfer occurs within the mixed-phase region, where the refrigerant absorbs latent heat. The linearity of the enthalpy gain in this region validates the consistent application of boiling correlations.
- Superheated Region: The trajectory exiting the saturation dome (where $x > 1.0$) confirms the onset of super-heating. This is a critical design check to ensure that the evaporator provides sufficient superheat to protect downstream compression equipment from liquid ingestion.

5.3 Local Heat Transfer Coefficients

A critical advantage of the discretized solver is the resolution of local heat transfer coefficients (HTC) along the coil length, rather than relying on a lumped-parameter average.

- **Boiling Regimes**: The solver distinguishes between nucleate boiling and convective boiling mechanisms. As vapour quality (x) increases along the tube, the flow transitions into annular regimes where convective forces dominate, typically enhancing the refrigerant-side HTC until dry-out occurs.
- **Pinch Point Analysis**: The temperature profile results highlight the approach temperature (pinch point) between the air and refrigerant. This local analysis ensures that the coil design avoids temperature crosses or ineffective zones where the driving temperature difference (ΔT) is minimal. The solver assumes that the heat transfer becomes zero in case the temperature difference between the refrigerant and air is negligible.

```
# From evap.py
            if T[u] >= localAirTemp[u] - 0.001:  # 0.001 tolerance for float
                precision
                Twall = localAirTemp[u]
                Qref = 0
            else:
                # Only run solver if there is a temperature difference
                def err(T_wall_guess):
                    Qguess = (
                        h_air
                        * (areaOuter / (nCircuits * nIter))
                        * (localAirTemp[u] - T_wall_guess)
                    )
                    Qref = h_ref * (math.pi * tubeID * dl) * (T_wall_guess - T[u])
                    return Qguess - Qref

                try:
                    # Use a slightly padded upper bound to avoid exact edge cases
                    sol = root_scalar(
                        err, bracket=[T[u], localAirTemp[u]], method="brentq"
                    )
                    Twall = sol.root
                    Qref = h_ref * (math.pi * tubeID * dl) * (Twall - T[u])
                except ValueError:
                    # Fallback if solver fails despite check (rare numerical noise
                        )
                    Twall = T[u]
                    Qref = 0
```

Listing 3: Fall-back code in case pinch-point is reached.

5.4 Pressure Drop and Hydraulic Performance

The hydraulic simulation isolates the two primary components of pressure drop: frictional loss and momentum change.

- **Two-Phase Friction**: The application of the Friedel multiplier accounts for the complex interaction between liquid and vapour phases. The results indicate that the majority of the pressure drop accumulates in the high-quality regions of the flow, where vapour velocity is highest.
- **Momentum Effects**: The acceleration pressure drop (ΔP_{mom}), resulting from the density decrease during phase change (liquid to vapour), is captured and added to the frictional losses to provide a total pressure drop value. This ensures the design remains within the allowable pumping head constraints of the system.

5.5 Temperature profile along the tube

The solver captures the temperature profile along the tube by mapping the temperature of the refrigerant against the distance in the tube. Figure 4.

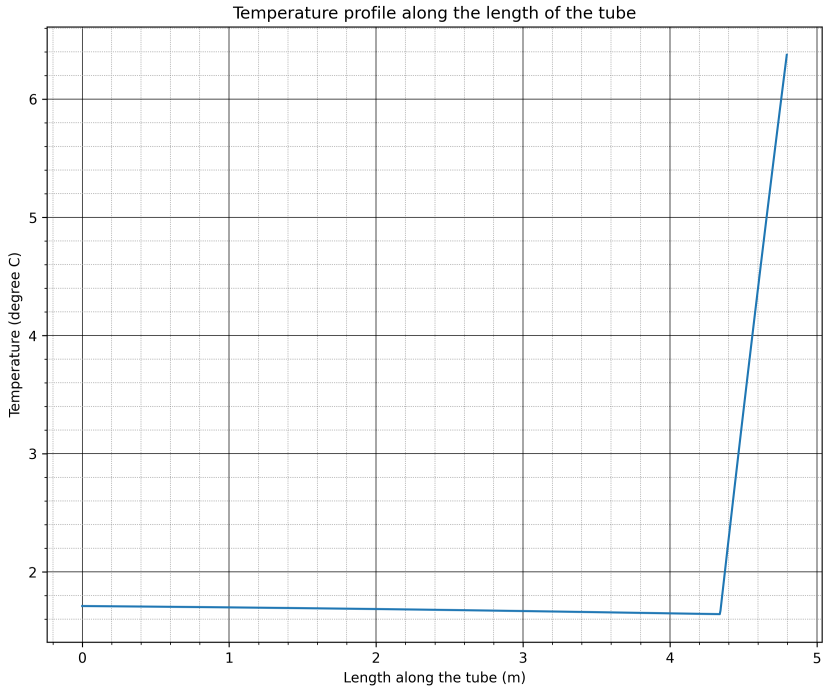

Figure 4: Temperature Profile along the length of the tube

A nearly constant saturation temperature is observed throughout the two-phase region as the temperature glide due to pressure drop is minimal in this high-pressure scenario. Upon transition to the superheated regime, the temperature increases distinctively, aligning with theoretical predictions for flow boiling.

6 Conclusions & Future Work

6.1 Summary of capabilities

This project successfully developed a Python-based, discretized finite-volume solver capable of simulating the thermal-hydraulic performance of staggered fin-and-tube evaporators. By moving beyond lumped-parameter assumptions, the tool provides high-fidelity insights into the coupled physics of air-side convection and refrigerant-side phase change.

Key capabilities of the developed solver include:

- Discretized Physics: The implementation of a segment-by-segment control volume approach allows for the resolution of local gradients in temperature, enthalpy, and vapor quality, identifying critical performance bottlenecks like pinch points.
- Robust Numerical Solution: The integration of `scipy.optimize` libraries (Brent's method) with custom iterative loops ensures energy balance convergence even under non-linear boiling regimes.
- State-Dependent Correlations: The solver dynamically selects appropriate heat transfer and pressure drop correlations (Wang et al. for air-side; nucleate/convective superposition for refrigerant-side; Friedel for two-phase friction) based on real-time flow regimes.
- Thermodynamic Rigor: Utilization of Helmholtz energy equations of state (via CoolProp) ensures that fluid properties remain accurate across the entire saturation dome and superheat regions.

6.2 Future Develpoment Roadmeap

While the current solver provides a robust baseline for plain-fin evaporator design, the modular architecture allows for significant functional expansion. Future development phases will focus on increasing physical fidelity and design flexibility:

- **Advanced Mass Transfer Modelling**: The current model approximates latent load handling via effective specific heat adjustments. A primary future objective is to implement a fully coupled heat and mass transfer model using the Enthalpy Potential method (or Lewis Relation). This would allow for rigorous prediction of dehumidification rates and condensate film thermal resistance on the fin surface.
- **Extended Surface Enhancement**: The geometric library, currently optimized for plain fins, will be expanded to include correlations for interrupted surfaces such as louvered, slit, and wavy fins. These surfaces are industry standards for compact heat exchangers and require distinct friction and Colburn j-factor correlations (e.g., Chang & Wang).
- **Inner Grooved Tube (IGT) Support**: To reflect modern HVAC&R trends, the refrigerant-side solver will be updated to account for the area enhancement and turbulence promotion of micro-fin tubes, rather than the current smooth-tube assumption.

7 References

[1] C.-C. Wang, K.-Y. Chi, and C.-J. Chang, "Heat transfer and friction characteristics of plain fin-and-tube heat exchangers, part II: Correlation," *International journal of heat and mass transfer*, vol. 43, no. 15, pp. 2693–2700, Aug. 2000, doi: 10.1016/S0017-9310(99)00333-6.

[2] W. M. Kays and A. L. London, *Compact Heat Exchangers*. Malabar, Fla: Krieger Pub Co, 1998.

[3] S. G. Kandlikar, "A General Correlation for Saturated Two-Phase Flow Boiling Heat Transfer Inside Horizontal and Vertical Tubes," *Journal of heat transfer*, vol. 112, no. 1, pp. 219–228, Feb. 1990, doi: 10.1115/1.2910348.

[4] S. Kandlikar, S. Garimella, D. Li, S. Colin, and M. R. King, *Heat Transfer and Fluid Flow in Minichannels and Microchannels*. Amsterdam, Netherlands San Diego, CA Oxford, UK: Elsevier Science, 2006.

[5] L. Friedel, "Improved Friction Pressure Drop Correlation for Horizontal and Vertical Two-Phase Pipe Flow," 1979.